Water Resour Manage (2010) 24:2721–2742
DOI 10.1007/s11269-010-9576-1

Value of Medium-range Precipitation Forecasts in Inflow Prediction and Hydropower Optimization

Guolei Tang · Huicheng Zhou · Ningning Li · Feng Wang · Yajun Wang · Deping Jian

Received: 2 January 2009 / Accepted: 5 January 2010 /
Published online: 26 January 2010

Abstract This paper presents an inflow-forecasting model and a Piecewise Stochastic Dynamic Programming model (PSDP) to investigate the value of the Quantitative Precipitation Forecasts (QPFs) comprehensively. Recently medium-range quantitative precipitation forecasts are addressed to improve inflow forecasts accuracy. Revising the Ertan operation, a simple hydrological model is proposed to predict 10-day average inflow into the Ertan dam using GFS-QPFs of 10-day total precipitation during wet season firstly. Results show that the reduction of average absolute errors (ABE) is of the order of 15% and the improvement in other statistics is similar, compared with those from the currently used AR model. Then an improved PSDP is proposed to generate monthly or 10-day operating policies to incorporate forecasts with various lead-times as hydrologic state variables. Finally performance of the PSDP is compared with alternative SDP models to evaluate the value of the GFS-QPFs in hydropower generation. The simulation results demonstrate that including the GFS-QPFs is beneficial to the Ertan reservoir inflow forecasting and hydropower generation dispatch.

Keywords Ertan reservoir · Quantitative precipitation forecasts · Global Forecast System · Inflow forecasting · Power generation dispatch

G.L. Tang (✉) · H.C. Zhou · F. Wang
Faculty of Infrastructure Engineering, Dalian University of Technology,
Dalian, 116023, Liaoning, China
e-mail: tangguolei@ gmail.com

N.N. Li
Department of Computer Science and Technology, Dalian Neusoft Institute of Information,
Dalian, 116023, Liaoning, China

Y.J. Wang · D.P. Jian
Ertan Hydropower Development Company, Ltd, Chengdu, 610021, Sichuan, China

1 Introduction

The Ertan hydropower station is one of the key power sources in the Sichuan electric network, located in the lower reaches of the Yalong River, in Sichuan province, southwest China. Currently used medium-range inflow forecasts are based on ARMA-type model (Auto-Regressive Moving Average model or Auto-Regressive model, Maceira et al. 1997), but rainfall, whether observed or forecasted, is not used. From the statistics of forecasting, ARMA-type model can be considered as an acceptable one for the dry season (from November to April of the following year) (Zhou et al. 2009). Recently, the Ertan station initiates efforts to improve inflow forecasts accuracy of the wet season by testing and comparing several inflow-forecasting models which make use of observed and predicted precipitation as input variables. As a first step, medium-range Quantitative Precipitation Forecasts (QPFs) over coming 10-day periods are addressed.

The use of QPFs from numerical weather prediction models as input data to run hydrological rainfall–runoff models, thereby obtaining extended inflow forecasts, has been explored by several authors (Yu et al. 1999; Ibbitt et al. 2000; Anderson et al. 2002; Jasper et al. 2002; Koussis et al. 2003; Habets et al. 2004; Collischonn et al. 2005, 2007). Collischonn et al. (2007) make predictions of medium-range reservoir inflow using the QPFs from the regional Era model run by the Brazilian Center for Weather Prediction applied to part of the Paranaiba river basin, and the results show forecast errors can be reduced considerably during both wet and dry season, compared with those from the ARMA model. And recent attempts have been made to consider the uncertainty in forecasts, using ensemble rainfall forecasts (Zhang et al. 2006; Bartholmes and Todini 2005; Goweleeuw et al. 2005) and to combine the inherent uncertainty of hydrological models with ensemble forecasts (Pappenberger et al. 2005). Krzysztofowicz and Henry (2001) present a Hydrologic Uncertainty Processor (HUP) which produces a probabilistic river stage forecast based on probabilistic QPFs. However, most of these results are from work that is still at the research stage, since operational forecasting systems still rely more on radar estimates and telemetry of measured rainfall or short-range nowcasting (Moore et al. 2005; Wang et al. 2005; Qiu et al. 2004; Yuan et al. 2008; Li and Lai 2004). Nevertheless, medium-range QPFs are gradually being introduced in operational inflow forecasting systems in an attempt to extend the range of forecasts (Bremicker et al. 2006; Moore et al. 2005), but value of the extended inflow forecasts using QPFs in hydropower generation should be further explored on a case-by-case basis, which is rarely addressed in the literature.

Hydropower operation can be represented mathematically as a stochastic, nonlinear optimization problem, as future inflows and energy demands are uncertain and the system dynamics are nonlinear (Kim and Palmer 1997). Despite intensive researches since the classic work of Young (1967), no generally applicable methods exist for solving reservoir operation problems. Rather, the choice of methods depends upon the characteristics of the reservoir system being considered and the specific objectives and constraints to be modeled. Stochastic dynamic programming (SDP) is particularly well suited to stochastic, nonlinear problems that characterize a large number of hydropower systems (Yeh 1985). In SDP, the hydrologic state variables translate various hydrologic information into the required probabilistic framework. Stedinger et al. (1984) developed a SDP model, which employed the

best forecast of the current period's inflow to define a reservoir release policy and to calculate the expected benefits from future operations. Karamouz and Vasiliadis (1992) proposed a Bayesian SDP (BSDP) incorporating a Bayesian approach within the SDP formulation. They stressed that flow transition probabilities from one month to the next can be updated as new forecasts become available. Such updating can significantly reduce the effects of natural and forecast uncertainties in SDP. Zhou et al. (2009) presents a hybrid SDP model (HSDP), that employs generated forecasts of inflow time series $\left\{Q_1^f, Q_2^f, \cdots, Q_{t^*}^f\right\}$ during dry season and a discrete lag-one Markov process during wet season as hydrologic state variables for the Ertan hydropower station, China. The simulation results demonstrate that including the best forecasts of inflow time series during dry season is beneficial in comparison to the standard operating policy.

The Global Forecast System (GFS) run by the American National Oceanic and Atmospheric Administration (NOAA) has made medium-range QPFs. However, the use of QPFs by the GFS (GFS-QPFs) as input into rainfall–runoff models is relatively undeveloped for medium-range reservoir inflow predictions (Zhou et al. 2009). In this paper, a global evaluation of the GFS-QPFs is done to explore the potential improvement in medium-range inflow predictions, and hydropower productions. Taking the Ertan hydropower station as an example, a simple hydrological model using GFS-QPFs is presented for forecasting the reservoir inflow during the wet season firstly, and the results from the proposed hydrological model will be compared with forecasts obtained by the currently used Auto-Regressive (AR) model quantitatively. Then an improved Piecewise SDP framework (PSDP) based on HSDP (Zhou et al. 2009) is proposed to generate operating policies for the Ertan station to better off incorporate inflow forecasts with various lead-times as hydrologic state variables. Finally performance of the PSDP model is compared with alternative stochastic programming models to evaluate the value of the GFS-QPFs in hydropower generation.

2 Study Site: The Ertan Hydropower Station

The case study in this paper is concentrated on the Ertan hydropower station. Figure 1 shows the location of the Ertan dam, and gauging stations. The Ertan dam is located in the lower reaches of the Yalong river basin in the Sichuan province of southern China. This part is relatively well covered with rain gauges and stream gauges, which transmit rainfall and flow at 6-h intervals in real time, as seen in Fig. 1. The Yalong river basin lies on the eastern edge of the Tibetan plateau that covers 26°32′–33°58′ N and 96°52′–102°48′ E, and the catchment area is about 136,000 km^2. The mean annual rainfall in catchment ranges is between 500 and 2,470 mm, and it is higher in the south and east. The area has two distinct seasons: dry and wet season, as its climate is mainly influenced by high-altitude westerly circulation and southwest Monsoon. Generally, this basin receives about 90% to 95% of the annual rainfall in the wet season (from May to October), while only 5% to 10% in the dry season (from November to April of the following year). So there is great possibility for hydropower improvement in the wet season. Over a period of 48 years the average annual inflow into the Ertan dam is 1,670 m^3/s. The transition of inflow in time period t to inflow in

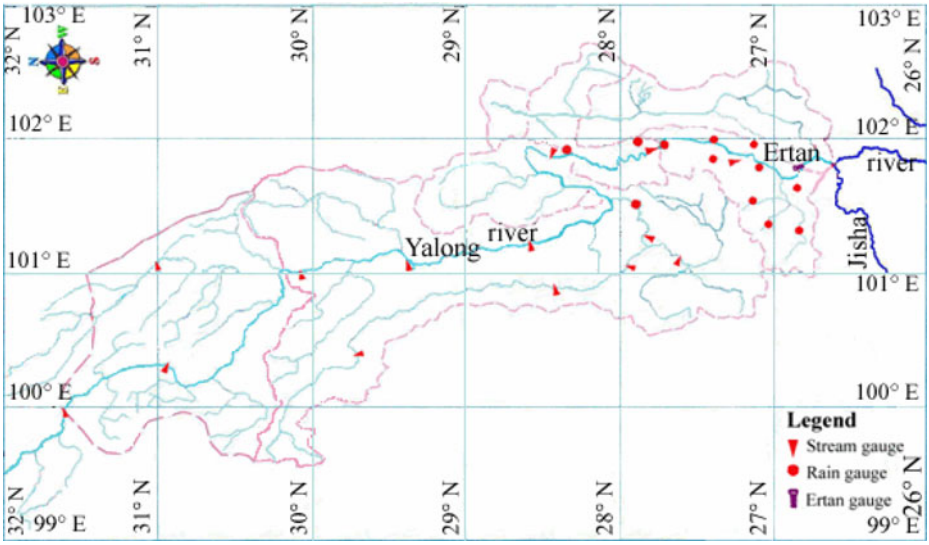

Fig. 1 Main features of the Yalong River basin and location of the Ertan dam and gauging stations

period $t + 1$ can be described by a first-order Markov chain using correlation analysis (Zhou et al. 2009).

The Ertan hydropower station is one of the key power sources for the Sichuan electric network, with an installed capacity of power generation of 3,300 MW through its power generation system composed by six hydro generators with an installed capacity of 550 MW each. Statistical analyses of actual data of the Ertan hydropower operation shows that, the wet season can be roughly divided into two periods by the features of underlaying surface and soil moisture content: the delivery period from early May[1] to mid June, and the storage period from late June to late October (Zhou et al. 2009). To meet the requirements of Ertan medium-range hydropower generation scheduling, reservoir operation model should be formulated for monthly operation during dry season and 10-day operation during wet season. Ertan operation policy is maximizing the total power supply, to make more profits by utilizing water resource rationally subject to the firm capacity of 1,028 MW committed for Ertan reservoir. The design reliability probability of hydroelectric generation of Ertan (Ertan DRPHG) is 95% (Zhou et al. 2009), which is the ratio of the number of periods the system output is satisfactory and the total number of running periods during the years of operation, and defined as the probability system's output is satisfactory (Hashimoto et al. 1982). More features are shown in Table 1, and the constrains including mass balance equation for the reservoir storage and inflow, releases from the reservoir, plant capability, turbine capacity and power productions; details are found in Zhou et al. (2009).

[1] In China, a month is divided into three periods: the first 10-day (early), the middle 10-day (mid) and the last 10-day (late) of a month. Taking May as an example, the first 10-day of May is denoted by early May, the middle 10-day of May is mid May, and the last 10-day of May is late May.

Table 1 Key descriptions of the Ertan hydropower station

Characteristic	Unit	Parameters
Dead storage capacity	Mm^3	2,430
Dead pool level	m	1,155
Gross storage capacity	Mm^3	5,800
Normal pool level	m	1,200
Usable storage capacity	Mm^3	3,370
Turbine capacity	m^3/s	2,400
Plant capability	MW	3,300
Firm capacity	MW	1,208
Minimum release	m^3/s	20
Power coefficient	–	8.6

3 Quantitative Precipitation Forecasts by Global Forecast System

The Global Forecast System run by NOAA is a global Numerical Weather Prediction (NWP) computer model, which produces QPFs up to 16 days at each data assimilation cycle (00, 06, 12 and 18 UTC) in advance, but with decreasing spatial and temporal resolution over time. The NWP model is run in two parts: the first part has a higher resolution and goes out to 180 h in the future; the second part runs from 180 to 384 h at a lower resolution. The resolution of the model varies in each part of the model: horizontally, it divides the surface of the earth into 35 or 70 km grid squares; vertically, it divides the atmosphere into 64 layers and temporally, it produces a forecast for every sixth hour for the first 180 h, after that they are produced for every 12th hour. The GFS is the only global NWP model for which all output including QPFs in GRIB1 format (Transited to GRIB2 since February 12, 2008) is available on NOAA FTP SERVERS for free over the internet, and as such is the basis for non-state weather companies, e.g., Wunderground.com, Weatheronline.co.uk, Weather.com.au, and t7online.com (GRIB 2008).

The GFS-QPFs over Continental United States (CONUS) have been evaluated by different measures including Equitable Threat Score (ETS), True Skill Statistics (TSS) and Bias. These statistics show that, the precipitation forecast has more skill in winter (December, January and February) when comparing to summer (June, July and August), and the skills have been improved gradually over the past several years when the model increased the resolution, improved analysis system and physical processes (Zhu 2007). The ETS is a good estimate for overall forecast skill, and has a range of −1/3 to 1. The higher the value of ETS, the better the forecast model skill is for that particular threshold. The TSS measures the ability of the forecasts to discriminate between "Yes" and "No" observations based on contingency tables (Doswell et al. 1990). It ranges from −1.0 (no correct forecasts) to 1.0 (perfectly correct). The Bias measures the relative frequency of predicted and observed rainfall. The best model is generally the one that remains near the 1.0 line. If the model verifies over 1.0, it is over-predicting precipitation, and if below 1.0 it is under-predicting precipitation.

Figure 2 are the objective scores of GFS precipitation skills over CONUS from Zhu (2007), for 00 UTC of August15, 2006 to 18 UTC of November 6, 2006 and 00 UTC of November 1, 2006 to18 UTC of February 5, 2007. Three different forecasts (12–36, 36–60, and 60–84 h, leading time) have been verified by calculating ETS, TSS and Bias. The x-axis is 24-h threshold precipitation amounts in mm. The numbers

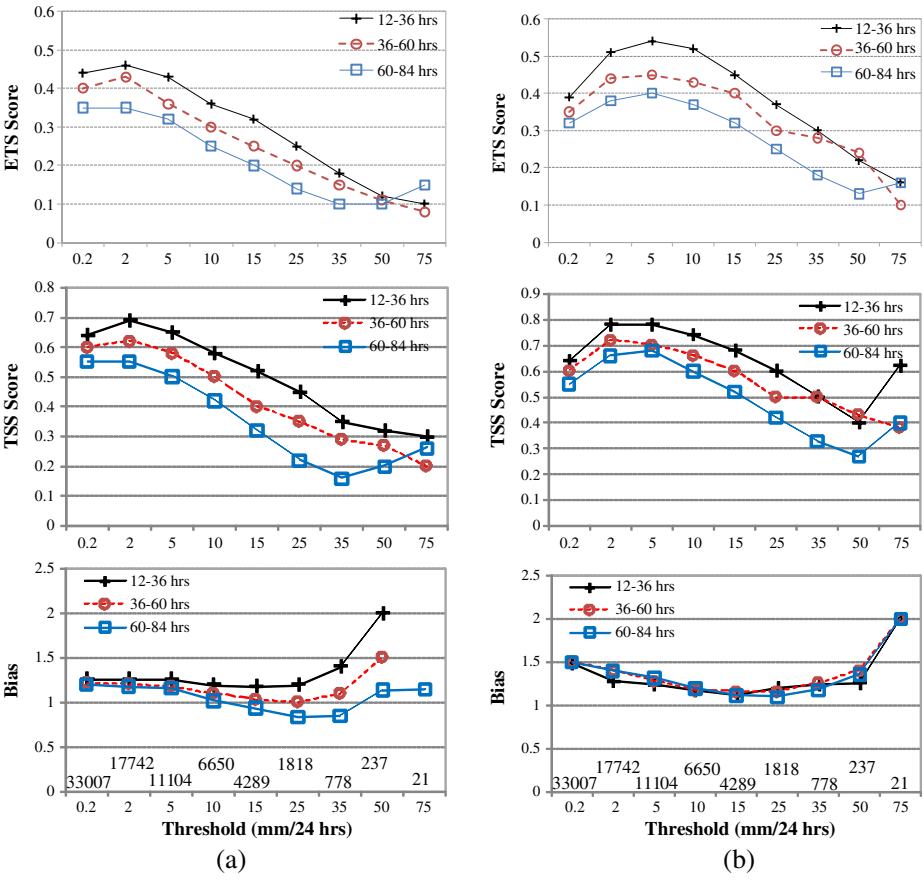

Fig. 2 The verification scores over CONUS including ETS, TSS and Bias are for (**a**) 00 UTC of August 15, 2006–18 UTC of November 6, 2006 and (**b**) 00 UTC of November 1, 2006–18 UTC of February 5, 2007

above *x*-axis are total observed grids/boxes in the verified period for that threshold. The Bias scores (Fig. 2a) are very similar at a range of 0.9 (10% under-forecast) to 2.0 (100% over-forecast) for all lead time forecasts, the TSS and ETS are reasonable decreasing their skills when increasing lead time. There is the same future for Fig. 2b except the Bias are less, TSS and ETS are larger. A more comprehensive description of GFS, including model parameters and its implementation changes, precipitation maps, and evaluation documentations is given by official website of NOAA.

The GFS-QPFs used in this study are the modeled precipitation forecasts over the entire East Asia region. A precipitation map published at 00 GMT July 15, 2006, is given in Fig. 3, showing the modeled precipitation in mm between 0 and 8 A.M. The precipitation areas are encircled by isohyets—lines with equal amounts of precipitation. For research purpose, the GRIB1 data sets are collected from the NOAA Server explained above during wet season from 2002 to 2006 firstly. Then the GFS-QPFs made at the first data assimilation cycle of 0000 UTC every day are extracted from the collected data sets for all gauging stations of the Yalong

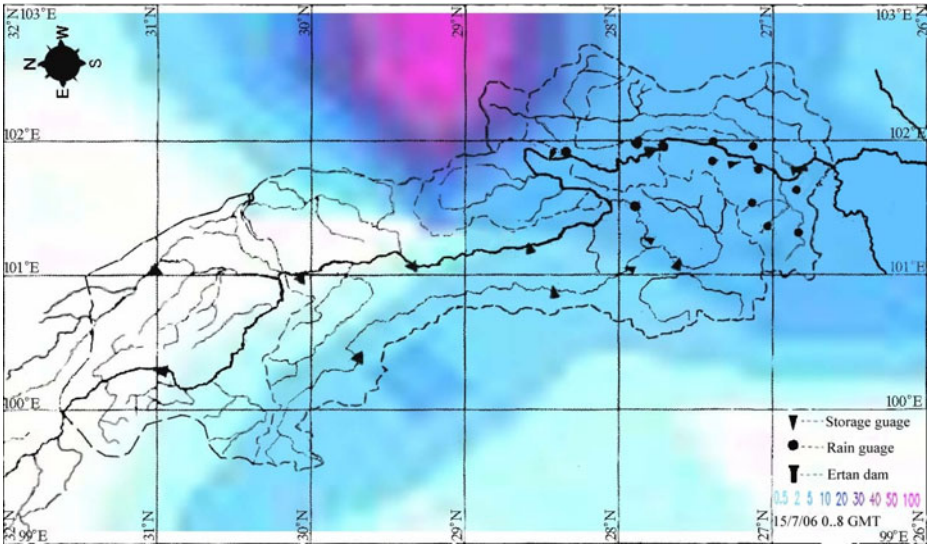

Fig. 3 Precipitation forecasting over the Yalong river basin at 00 GMT July 15, 2006

river basin shown in Fig. 1, by a GRIB1 Encoder/Decoder program, which also can be downloaded from GRIB (2008). Finally, the observed and forecasted average areal precipitations for the next 10 days in Yalong river basin (termed by 10-day subsequent precipitations) are estimated by the Thiessen polygon method (McCuen 1998), which assigns an area called a Thiessen polygon to each station in the Yalong river basin shown in Fig. 1. The practical use of the collected 10-day subsequent GFS-QPFs over the Yalong river basin will be discussed in the following sections in details.

4 Inflow Forecasting Model

4.1 A Rainfall–Runoff Model Using Quantitative Precipitation Forecasts

Many hydrological models can be used to predict reservoir inflows using the quantitative precipitation forecasts, and the comparative study should include lumped rainfall–runoff models (Reed et al 2004), and more complex Distributed Hydrological Models (DHM, Collischonn et al. 2005, 2007). However, the input data guiding the DHM or physically-based lumped models' parameter calibration including land use, topography, vegetation cover and soil types (Beven 2001), is not available at all as collecting such data is too expensive (Zhou et al. 2009). So the results presented in this paper are all obtained by a simpler lumped Rainfall–Runoff model using GFS-QPFs (denoted by GRR). The GRR model incorporates with the forecasts of 10-day subsequent precipitation by the Thiessen polygon method (McCuen 1998), published at 00 UTC the first day of every 10 days, e.g. May 1, May 11 and May 21 during the month of May, as an input variable. Further researches on forecasting inflows using the DHM should be done as the data become available.

As mentioned in Section 2, the wet season can be roughly divided into two periods by the features of underlaying surface and soil moisture content, so the GRR model is a two-segment multi-factor inflow forecasting model. Model configuration is estimated by the stepwise regression algorithm (Sun et al. 1998) using observed and forecasted hydrological data from the Ertan reservoir during the wet season from 2002 to 2005, and verified using data of 2006. And predictors P_t^f, P_{t-1} and Q_{t-1} are chosen to predict inflows to Ertan dam. So it is given as a piecewise function in Eq. 1:

$$Q_t = \begin{cases} -165.1 + 1.01P_t^f + 15.17P_{t-1} + 1.16Q_{t-1} & 1 \le t \le 5 \\ 173.1 + 13.84P_t^f + 4.87P_{t-1} + 0.56Q_{t-1} & 6 \le t \le 18 \end{cases} \quad (1)$$

where Period t is reckoned 1, 2, 3,..., 18 in the forward direction, and $t = 1$ denotes a 10-day period starting on May 1st while $t = 18$ denotes the period ending on October 31st; Q_t is the modeled 10-day inflow in cubic meters per second to Ertan dam for period t using the model; P_t^f is the estimated 10-day subsequent accumulated GFS-QPFs in mm during period t by the Thiessen polygon method (McCuen 1998); P_{t-1} is observed 10-day total precipitation in mm during previous period $t-1$ also estimated by the Thiessen polygon method; Q_{t-1} is observed 10-day average inflow in cubic meters per second to Ertan dam of previous period $t-1$.

4.2 Quantitative Analysis of Inflow Forecasting Models

Predicted 10-day average inflows into the Ertan dam obtained by the GRR model using GFS-QPFs are compared with forecasts by the currently-used AR model. Figure 4 presents the hydrographs of observed and predicted 10-day average inflows during the wet season from 2002 to 2006. It can be seen that forecasts obtained by the GRR model are closer to observed inflow in most cases, especially for the first five periods each year, which correspond to the end of the recession of the dry season, and for the rising parts of the hydrograph. The AR forecasts show a pattern of a one 10-day delay with maximum and minimum values postponed by one 10 days, which is a consequence of the model structure. The value of including new information given by rainfall forecasts can also be seen during periods when the hydrograph is rising

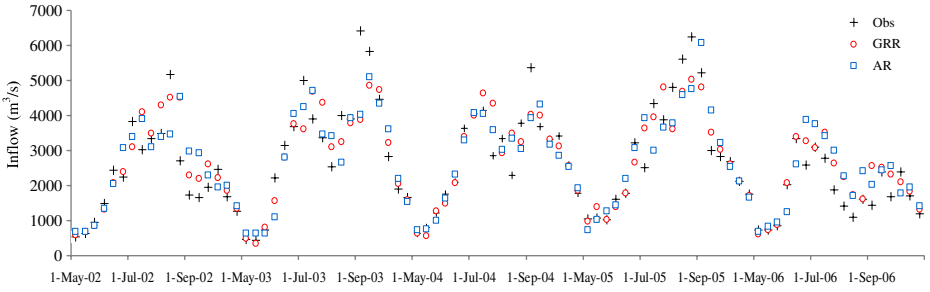

Fig. 4 Hydrographs of observed and predicted 10-day average inflows during wet season from 2002 to 2006

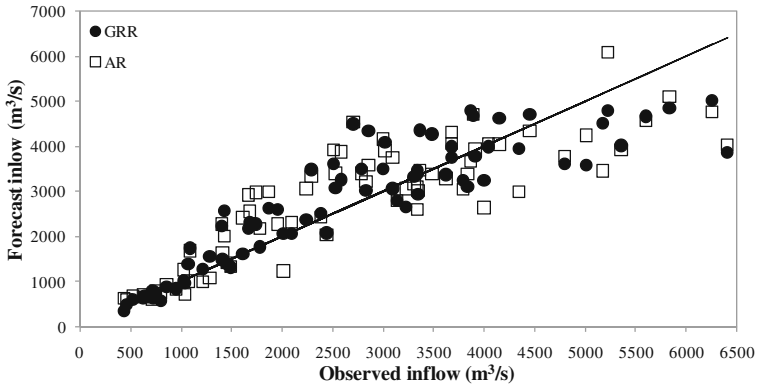

Fig. 5 Scatter plot of observed versus predicted 10-day averages of inflows using the GRR model with rainfall forecasts and the AR model

and during sharp changes in inflow when the hydrograph may increase or decrease, which is consistent with that from Collischonn et al. (2007).

Figure 5 compares observed and predicted 10-day average inflows into the Ertan dam considering both the GRR hydrological model using GFS-QPFs and the currently used AR model during the wet season from 2002 to 2006. For low inflows both forecasting models perform relatively well, with points representing the GRR forecasts rather closer to the line of perfect forecasts. For inflows larger than 1,500 m^3/s, both forecasting models do not perform well, though points are considerably more dispersed with a less pattern of larger dispersion for the AR model, most of which occurs in the main flood season from late June to late September, and there is a dramatic change in the inflows as seen from Fig. 4. For example, the average inflows in August vary greatly over the last 49 years from 1958 to 2006: the minimum inflow is about 1,200 m^3/s, while the maximum inflow is approaching 7,200 m^3/s, which makes it hard to get perfect forecasts of inflow during main flood season. In some cases, however, it is not necessary to have very accurate forecasts, since relatively rough estimates can improve the operation of hydraulic structures, or can yield estimates of the risk that rivers will exceed specified discharge thresholds (Rabuffetti and Barbero 2005), especially for forecasts of inflows into reservoirs in the medium range. So qualitative analysis of 10-day inflow forecasts using the GRR model will be further made for evaluation tasks in the following sections.

Table 2 Error statistics for 10-day average inflow forecasts obtained by the GRR model using rainfall forecasts and forecasts obtained by the AR model for both calibration and verification

Statistics	AR model		GRR model	
	Calibr.	Verific.	Calibr.	Verific.
Average absolute error (ABE)	577	616	526	389
Average relative error (ARE)	21	33	17	24
Root mean square error (RMSE)	792	723	738	542
Nash–Sutcliffe efficiency (NSE)	0.75	0.63	0.79	0.79

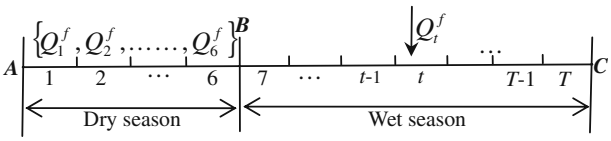

Fig. 6 Available hydrologic state variables for dry season (AB) and wet season (BC)

Several error analyses compare forecasts obtained by the GRR model with QPF as inputs with forecasts by the AR model for both calibration (from 2002 to 2005) and verification (the year 2006). The results are given in Table 2, showing that the GRR model performs better in all cases, no matter for calibration or verification. The reduction of average absolute errors (ABE) is of the order of 15% and the improvement in other statistics is similar. It is not possible to assert at present whether this improvement results in better decisions in reservoir operation, however we expect that better forecasts will probably lead to better decisions.

4.3 A Summary of Available Hydrological State Variables

The qualitative forecasts of 10-day average inflow using GRR model might assist the decision maker in selecting the better reservoir operating policy for the Ertan reservoir. Then the Markov-type inflow process during wet season in HSDP (Zhou et al. 2009) will be updated by anew forecasts of current period's inflow, and a relatively new model for inflow process is formed as illustrated in Fig. 6. The model includes forecasts of monthly inflow series $\left\{Q_1^f, Q_2^f, \cdots, Q_6^f\right\}$ with lead-times of 6 months during the dry season (Zhou et al. 2009), and 10-day average inflow forecasts Q_t^f with one 10-day lead-time during wet season. The potential value of available inflow forecasts to long-term water system operations may be significant if there are modeling techniques and decision processes available to exploit them. So next section will focus on the development and evaluation of decision support models that can be used in real time, and employing the predicted inflows with various lead-times as hydrologic state variables to determine the most efficient operating decisions.

In many cases, it is computationally convenient to represent state variables as a number of discrete values known as characteristic values, such as characteristic storages and characteristic inflows (Karamouz and Vasiliadis 1992). The storage state variable, Ertan beginning storage, is discretized into 23 characteristic values using the Savarenskiy's scheme (Klemes 1977). The inflow and forecast are assumed to be log-normally distributed and then discretized with 3 characteristic values by using the nonuniform symmetric scheme (Kim and Palmer 1997).

5 Reservoir Optimization Model and Its Application

5.1 Objective Function

As previously stated, Ertan operation policy should not only maximize the total power supply to make more profits but also produce the firm power as far as possible to guarantee power system stable running and peak-load regulation especially during

dry season. So the system performance considered should be a penalty function for a given combination of available state variables S_t, H_t and decision variable, S_{t+1}. Once the calculated power generation $P(\cdot)$ in MW is less than the firm power of 1,028 MW, the reservoir system must be "punished", and the value of system performance measure $B(\cdot)$ in gigawatt hour will decrease correspondingly, determined by the penalty factors α and β. Thus the objective function, a maximization function can be written as:

$$f_{opt}^{n}(S_t, H_t) = \underset{S_{t+1}}{Max}\left[\sum_{t=1}^{T} E\left[B(S_t, H_t, S_{t+1})\right]\right] \forall S_t, H_t, \{\text{feasible } S_{t+1}\} \tag{2}$$

$$B(S_t, H_t, S_{t+1}) = \left[P(S_t, H_t, S_{t+1}) - \alpha \cdot \left\{\max\left(P(S_t, H_t, S_{t+1}) - 1028, 0\right)\right\}^{\beta}\right] \cdot \Delta t \tag{3}$$

where $f_{opt}^{n}(\cdot)$ is the maximum expected generation of hydropower system return from the current period to the end of the planning horizon; t is the index of time period, and $t = 1, \ldots, T$; n is the number of time period remaining until the end of the planning horizon; S_t is the storage at the beginning of period t (termed by beginning storage); S_{t+1} is the target storage at the end of the period t (termed by end storage); H_t is hydrologic state variables for period t, such as class interval or point value of inflow forecast during period t, inflow during the previous period $t-1$ and so on; α and β are the penalty factors determined by Ertan DRPHG; Δt is the time in hours for decision interval t.

5.2 Classical Stochastic Dynamic Programming

In classical SDP models, the optimal reservoir end storage for time period t can be determined by solving the following recursive equation (Tejada-Guibert et al. 1995):

$$f_{opt}^{n}(S_t, H_t) = \underset{S_{t+1}}{Max}\left\{E_{Q_t|H_t} \cdot B_t(S_t, Q_t, S_{t+1}) + E_{Q_t|H_t} \cdot E_{H_{t+1}|H_t, Q_t} \cdot f_{opt}^{n-1}(S_{t+1}, H_{t+1})\right\} \tag{4}$$

where Q_t is the inflow during current period t; and $E_{Q_t|H_t}$ is the conditional expectation operator for a flow of Q_t during period t, given a specific H_t during period t.

5.3 Alternative SDP Models for Hydropower Operation

Four alternative SDP models can be formulated from Eq. 4, each employing a different set of hydrologic state variables. The differences between the alternative SDP models depend on how the hydrologic state variables are defined as well as the expectation operators used in Eq. 4. This paper compares the operation policies derived by the alternative SDP models to measure the value of using various hydrologic information, and also with the proposed PSDP policies to measure the value of including current flow forecasts using medium-range quantitative precipitation forecasts from Global Forecast System.

Let i be the class interval of inflow Q_{t-1} in previous period $t-1$; k be the class interval of inflow forecast Q_t^f in current period t; j be the class intervals of inflow Q_t in current period t; and l be the class intervals of inflow forecast Q_{t+1}^f of next period $t+1$, and h be the class intervals of inflow Q_{t+1} of next period $t+1$.

Deterministic Dynamic Programming (DDP) does not consider any stochasticity of inflow processes. In DDP, it is assumed that a given sequence of inflow repeats infinitely. DDP with perfect forecast time series used in this study is expected to be superior to any SDP and provides a base against which is to compare the value of stochastic models, and to explore how to further increase the efficiency of power generation. Because DDP uses no hydrologic state variable, Eq. 4 can be reduced to:

$$f_{opt}^{n}(S_t) = \underset{S_{t+1}}{Max}\left\{B_t(S_t, Q_t, S_{t+1}) + f_{opt}^{n-1}(S_{t+1})\right\} \tag{5}$$

where Q_t is the historical flow in time period t.

Another alternative DP model, denoted SDP-Q, includes the previous period's inflow $Q_{t-1} = i$ as a hydrologic state variable, as illustrated in Fig. 7a. It allows

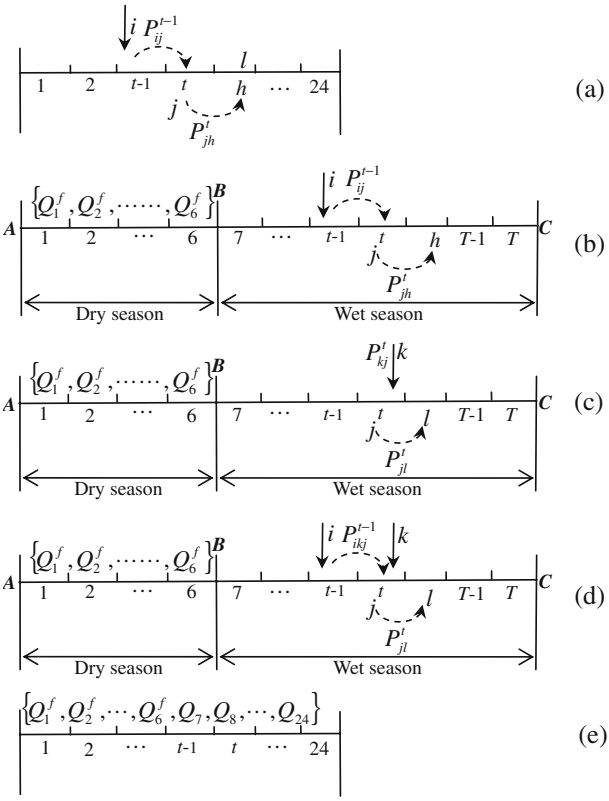

Fig. 7 The evaluation process from (**a**) SDP-Q to (**b**) HSDP, (**c**) HSDP-F, (**d**) PSDP and (**e**) DP, each employing a different set of hydrologic state variables

inclusion of the serial correlation between two consecutive periods. Thus, Eq. 4 becomes:

$$f_{opt}^{n}(S_t, i) = \underset{S_{t+1}}{Max} \left\{ \sum_j P_{ij}^{t-1} \cdot \left(B_t(S_t, j, S_{t+1}) + \sum_l P_{jh}^{t} \cdot f_{opt}^{n-1}(S_{t+1}, h) \right) \right\} \quad (6)$$

The third alternative DP model, denoted HSDP (Zhou et al. 2009), a combination of DDP and SDP-Q, includes predicted inflow time series using ARMA forecasting model during dry season and the previous period's inflow $Q_{t-1} = i$ during wet season as hydrologic state variables, as shown in Fig. 7b. More details of the HSDP model and its recursive equation are also found in Zhou et al. (2009).

The last alternative DP model, denoted HSDP-F, employs the current period's inflow forecast $Q_t^f = k$ as a hydrologic state variable, and the likelihood probability P_{kj}^t to address the randomness of the inflow, as illustrated in Fig. 7c. Thus:

$$f_{opt}^{n}(S_t, k) = \underset{S_{t+1}}{Max} \left\{ \sum_j P_{kj}^{t} \cdot \left(B_t(S_t, j, S_{t+1}) + \sum_l P_{jl}^{t} \cdot f_{opt}^{n-1}(S_{t+1}, l) \right) \right\} \quad (7)$$

5.4 Proposed Piecewise SDP model

A PSDP model is proposed to better off incorporating available inflow forecasts at different lead-times, and the recursive equations of which vary from period to period. The outline of the model is depicted in Fig. 7d. The randomness of the inflow is addressed through a posterior transition probability P_{ikj}^{t-1}, and the uncertainty in flow forecasts is addressed through both the posterior flow transition probability P_{ikj}^{t-1}, and the predictive probability of forecasts P_{jl}^{t}. These two probabilities together handle the inflow uncertainty and forecast uncertainty. Time horizon for which decisions need to be obtained is a year, with months for dry season and 10 days for wet season taken as stages. P_{ikj}^{t} and P_{jl}^{t+1} are evaluated by a relative frequency approach as illustrated in Kim and Palmer (1997).

The posterior flow transition probability P_{ikj}^{t-1}, gives the probability that the flow Q_t in time period t belongs to the class interval j, given that the flow Q_{t-1} in time period $t-1$ belongs to class interval i and the forecast Q_t^f for flow in time period t, belongs to class interval k. It is the revised inflow transition probability, derived using Bayesian Decision Theory (Mayer 1970, Eq. 8), by incorporating new information, a forecast Q_t^f for current period t, to the prior inflow transition probability P_{ij}^t and likelihood probability P_{kj}^t:

$$P_{ikj}^{t} = P\left[Q_t = j \middle| Q_t^f = k, Q_{t-1} = i \right] = \frac{P\left[Q_t^f = k \middle| Q_t = j \right] \cdot P\left[Q_t = j \middle| Q_{t-1} = i \right]}{\sum_{Q_t} P\left[Q_t^f = k \middle| Q_t \right] \cdot P\left[Q_t \middle| Q_{t-1} = i \right]} \quad (8)$$

The predictive probability of forecasts P_{jl}^{t}, gives the probability that the forecast Q_{t+1}^f for flow in the time period $t+1$ belongs to class interval l, given that the flow Q_t in previous period t belongs to class interval j. It predicts the uncertain forecast Q_{t+1}^f for

the next period $t+1$ from the inflow Q_t during period t, determined from the Total Probability Theorem (Mayer 1970, Eq. 9). This links the inflow Q_t in the period t, to forecast Q_{t+1}^f in the next period $t+1$, in PSDP recursive equation (Eq. 10):

$$P_{jl}^{t+1} = P\left[Q_{t+1}^f = l \middle| Q_t = j\right] = \sum_{Q_{t+1}} P\left[Q_{t+1}^f = l \middle| Q_{t+1}\right] \cdot P\left[Q_{t+1} \middle| Q_t\right] = j] \quad (9)$$

Thus, the recursive equation for the period $t > 6$ and stage $n < 19$ during wet season can be written as:

$$f_{opt}^n(S_t, i, k) = \underset{S_{t+1}}{Max} \left\{ \sum_j P_{ikj}^t \cdot \left(B_t(S_t, j, S_{t+1}) + \sum_l P_{jl}^{t+1} \cdot f_{opt}^{n-1}(S_{t+1}, j, l) \right) \right\} \quad (10)$$

When the computations proceed to the period $t^* = 6$ and $n^* = 19$ (Point ***B***, Fig. 6) in backward recursive, accurate quantitative inflow forecast Q_{t^*} for time period t^* is given. For the current period t^*, the system performance measure is known to be B_{t^*} for given values of S_{t^*}, j and S_{t^*+1}. The expected value of system for the subsequent periods is calculated from $P_{jl}^{t^*+1}$, and $f_{opt}^{n^*-1}(S_{t^*+1}, j, l)$, calculated by the recursive Eq. 9 for the period t^*+1 for a given combination of j and l, so the recursive equation for period t^* and stage n^* is given as:

$$f_{opt}^{n*}(S_{t^*}, j) = \underset{S_{t^*+1}}{Max} \left\{ B_{t^*}(S_{t^*}, j, S_{t^*+1}) + \sum_l P_{jl}^{t^*+1} \cdot f_{opt}^{n^*-1}(S_{t^*+1}, j, l) \right\} \quad (11)$$

Table 3 Hydrologic state variables and conditional probabilities for dry and wet season in various SDP models

Figure	SDP models	Hydrologic state variable		Conditional probabilities	
		Wet season	Dry season	Wet season	Dry season
7a	SDP-Q	Q_{t-1}^f	Q_{t-1}^f	P_{ij}^{t-1}, P_{jh}^t	P_{ij}^{t-1}, P_{jh}^t
7b	HSDP	Q_{t-1}^f	$\left\{Q_1^f, Q_2^f, \cdots, Q_6^f\right\}$	P_{ij}^{t-1}, P_{jh}^t	E^1
7c	HSDP-F	$Q_t^{f_2}$	$\left\{Q_1^f, Q_2^f, \cdots, Q_6^f\right\}$	P_{kj}^{t-1}, P_{jl}^t	E
7d	PSDP-AR	$Q_{t-1}^f, Q_t^{f_3}$	$\left\{Q_1^f, Q_2^f, \cdots, Q_6^f\right\}$	P_{ikj}^{t-1}, P_{jl}^t	E
7d	PSDP-GRR	$Q_{t-1}^f, Q_t^{f_2}$	$\left\{Q_1^f, Q_2^f, \cdots, Q_6^f\right\}$	P_{ikj}^{t-1}, P_{jl}^t	E
7e	DDP	$\{Q_7, Q_8, \cdots, Q_{24}\}$	$\{Q_1, Q_2, \cdots, Q_6\}$	E	E

(1) $E = \begin{bmatrix} 1 & 0 & \cdots & 0 \\ 0 & 1 & \cdots & 0 \\ \vdots & \vdots & & \vdots \\ 0 & 0 & \cdots & 1 \end{bmatrix}$. If the forecasts are perfect, the likelihood P_{kj}^{t-1} matrix, which presents the forecast uncertainty, will get reduced to an identity matrix. Thus, the posterior flow transition probability matrix, which is a function of the likelihood matrix, will get transformed to a matrix containing only 1.0 and 0.0 entries in a symmetrical arrangement. (2) Q_t^f in HSDP-F and PSDP-GRR models is the inflow forecast by GRR model. (3) Q_t^f in PSDP-AR is the inflow forecast by AR model

When the computations proceed to the next period $t^* - 1$ in backward recursive, quantitative inflow forecasts and for period $t^* - 1$ and t^* are both given, so the state variables of the reservoir will include the reservoir stage class intervals at the beginning of period $t^* - 1$, S_{t^*-1}, and point value of inflow forecast into the reservoir during period $t^* - 1$, , then the recursive equation for period $t^* - 1$, can be written:

$$f_{opt}^{n}(S_t, k) = \underset{S_{t+1}}{Max} \left\{ B_t(S_t, k, S_{t+1}) + f_{opt}^{n-1}(S_{t+1}, l) \right\} \tag{12}$$

5.5 A Summary of Reservoir Optimization Models

Table 3 shows the hydrologic state variables for dry and wet season required in various SDP models. In each case, the conditional expectation is evaluated with conditional probabilities including flow and forecast transition probabilities, as also presented in Table 3.

6 Results and Discussion

6.1 Generation of Steady-State Operating Policies

Using backward recursion, each SDP model is run iteratively until the ending storage reach steady state. The generated operating policy is considered to be in the steady state when the expected average annual total power generation becomes constant for all periods and all combinations of the discretized state variables, and the obtained reliability probability of hydroelectric generation of Ertan from simulation results by a relative frequency approach should be 95% to guarantee power system stable running and peak-load regulation during dry season. Using this convergence criterion, DDP, SDP-Q, HSDP, HSDP-F, PSDP-AR and PSDP-GRR models require 4, 5, 7, 8, 9 and 9 iterations, respectively, to generate the steady-state operating policy. Figure 8 shows a typical PSDP policy plot derived by PSDP model using GRR forecasting model in early August ($t = 15, \alpha = 1$, and $\beta = 2.5$). From the policy, the optimal Ertan end storage S_{16} can be obtained for a given combination of state variables including Ertan beginning storage S_{15}, i and k, where i is the class

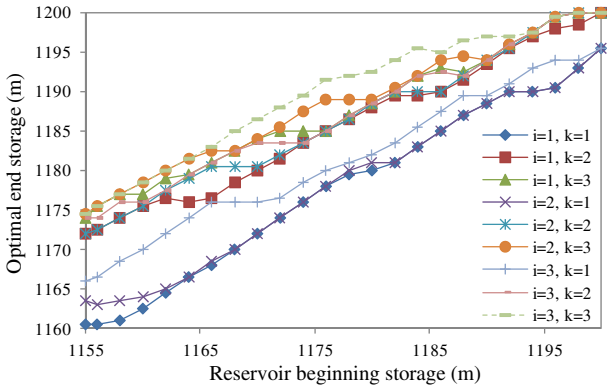

Fig. 8 A typical policy plot derived by PSDP-GRR model in early August for the Ertan reservoir

interval of inflow to the reservoir during late July; k is the class interval of inflow forecast during early August.

6.2 Simulation for Hydropower Generation Policies

The simulation analysis investigate the hydropower system performance when the operating policies derived from the proposed SDP models are employed in operation, using historical or synthetic flows and forecasts. Four performance indicators chosen to study the performances of the system under a given steady state operating policy and assist decision makers in selecting the best reservoir operating policy are: Annual Total Hydropower Generation (denoted by ATHG), Nash–Sutcliffe Sufficiency Score (NSSS), reliability, and vulnerability (Zhou et al. 2009). ATHG of the system is the target value of optimal operation, so it is the most important of these four indicators. NSSS is often defined as the ratio of the mean square error to the variance in the observed data, subtracted from unity. It is used here to measure how the storage hydrograph obtained by a given policy (termed by obtained storages) coincide well with the perfect storage hydrograph (termed by perfect storages) gotten by DDP with historical inflows time series as input, and higher values of which indicates better agreement between the obtained storages and perfect storages. The discussion about the last two indictors is taken from Suresh (2002) and Vijaykumar et al. (1996). Reliability of the system under a given policy is defined as the probability that the system output is satisfactory (Hashimoto et al. 1982). The last indicator, vulnerability of the system under a given policy is defined as the ratio of the average of the largest deficit occurring in the year for the system to the firm power committed for the system. Vulnerability gives a measure of how large is the deficit. In order to determine a specific performance indicator for a given policy, the system is simulated over several years.

6.3 Simulation Results

Optimal operation policies for Ertan station have been derived with an objective function that maximizes the expected value of total power generation with the firm power committed for Ertan station. The performance of the Ertan reservoir should desirably result in high values for ATHG and reliability and low values for vulnerability. Table 4 presents the simulation results of the alternative SDP models as well as the proposed PSDP model using the predicted inflows by the AR and GRR model with the rainfall forecasts from GFS during wet season respectively.

Table 4 Performance indicators for the various operating polices

Operating policy	Performance indicators			
	ATHG (GWh)	NSSS (%)	Reliability (%)	Vulnerability (%)
SDP-Q	16,526	0.72	98.71	1.78
HSDP	16,758	0.79	95.15	4.45
HSDP-F	17,086	0.80	95.11	3.83
PSDP-AR	17,092	0.82	95.17	3.67
PSDP-GRR	17,106	0.92	95.12	2.59
DDP	17,540	1	95.02	1.46

In general, the more sophisticated the model, the better its performance. However, marginal benefits of improved models are different:

(1) HSDP performs considerably better than SDP-Q, which shows that incorporating the predicted inflow time series during the dry season is considerably beneficial. The forecasts for inflow time series during dry season employed as a hydrologic state variable are so perfect, that the likelihood matrix, which presents the forecast uncertainty, gets reduced to an identity matrix. Then, the corresponding conditional probabilities P_{ij}^{t-1} and P_{jh}^{t} of SDP-Q, will transform to a matrix containing only 1.0 and 0.0 entries in a symmetrical arrangement in HSDP model, which result in appreciable improvements.

(2) PSDP-AR, HSDP-F and PSDP-GRR perform considerably better than HSDP, which shows that adding the predicted current period's inflow during wet season as another hydrologic state variable is also obviously beneficial. Figure 9 shows prior flow transition probabilities for late July, when the lag 1 autocorrelation is 0.52. Figure 10 shows the posterior flow transition probabilities used in PSDP for all cases (Low, Medium, and Large) of the one 10-day-ahead inflow forecasts obtained by GRR and AR model in early May and late July. The comparisons show that employing the forecasts for current time period's inflow, especially those obtained by GRR model as a hydrologic state variable in PSDP, lead to differences between the prior and posterior flow transition probabilities to a certain extent.

(3) PSDP-GRR performs much better than PSDP-AR, which shows that employing the predicted current inflow obtained by GRR model with the QPFs from GFS as a hydrologic state variable during wet season, results in higher values of ATHG (approximately 114 GWh), NSSS, and reliability, and in a lower value of vulnerability, compared to employing that obtained by the AR model. The prior flow transition probability matrix plays the governing role in DP algorithm such as SDP-Q and HSDP during wet season. On another hand, the posterior and predictive probability matrix, are functions of the likelihood matrix, and when the forecasts are not perfect, the likelihood matrix plays the governing role, and through Bayesian law, incorporates the forecast uncertainty in PSDP during wet season. Figure 11 shows the likelihood probabilities for both GRR and AR inflow forecasting models. For GRR model, the diagonal probabilities are larger compared to that of AR model because of the higher forecasting

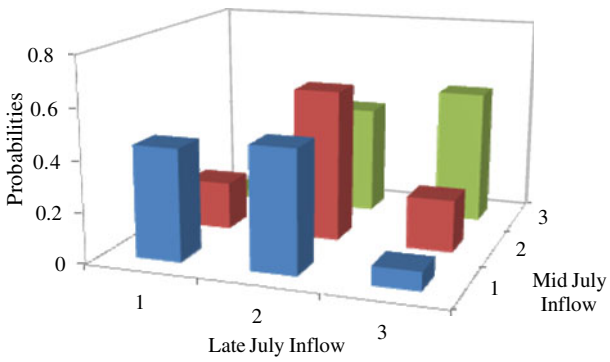

Fig. 9 Prior flow transition probabilities for late July

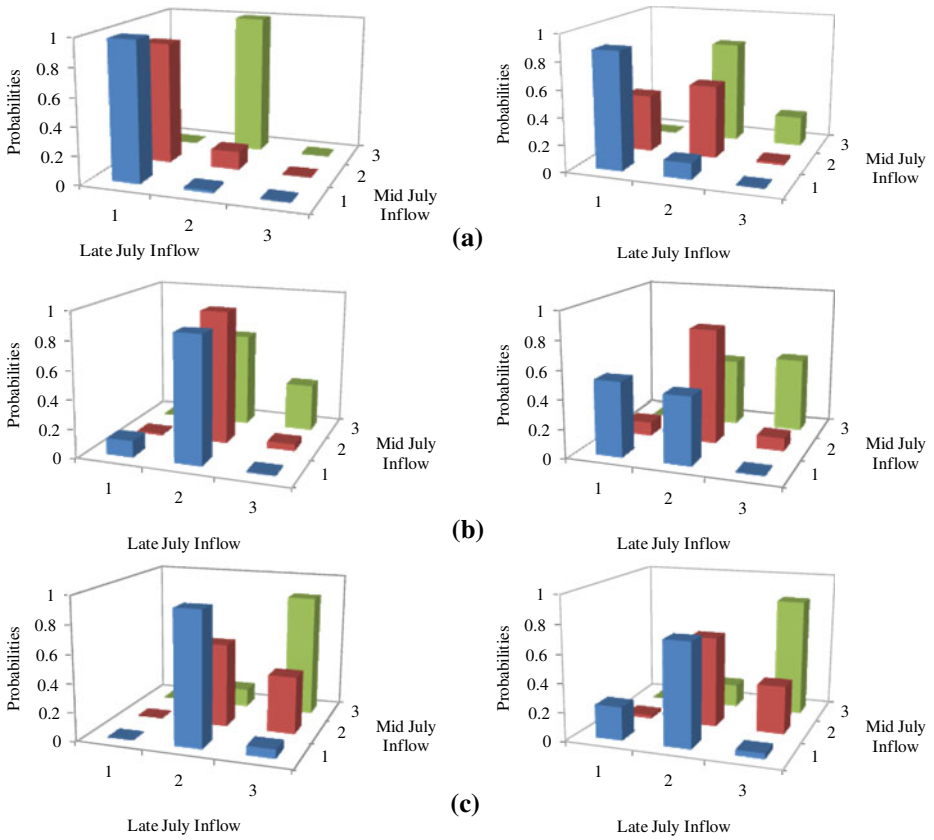

Fig. 10 Posterior flow transition probabilities for late July using the predicted current inflows (**a**) low; (**b**) medium; (**c**) large by both GGR model and AR model

accuracy of GRR, so PSDP-GRR policies results in better decisions, and better forecasts indeed lead to higher benefits. The comparison of performances from simulation for given operating policies fully proves that value of medium-range quantitative precipitation forecasts from Global Forecast System in inflow

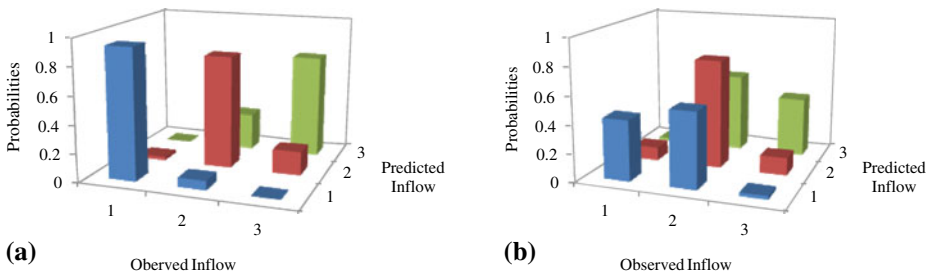

Fig. 11 Likelihood probabilities for (**a**) GRR; (**b**) AR forecasting models

Table 5 Average hydropower generation during both dry and wet season for PSDP-GRR and HSDP policies

Operating policy	AHPG (GWh)		
	A whole year	Dry season	Wet season
PSDP-GRR	17,106	5,005	12,101
HSDP	16,758	4,622	12,136
DDP	17,537	5,102	12,435

forecasting and power generation dispatch of the Ertan hydropower station, and the PSDP-GRR policy is chosen to optimize the Ertan reservoir operations in this study.

Meanwhile, Table 5 shows the value of Average Hydropower Generation (AHPG) within dry season for PSDP-GRR is 385 GWh higher than that for HSDP, but the value of AHPG within wet season for PSDP-GRR is 35 MkWh lower than that for HSDP. The findings seem to contradict the fact that the HSDP policy during wet season is improved by introducing the predicted current inflow as a hydrologic state variable. To seeking the answers, the storage hydrographs obtained using PSDP-GRR, HSDP and DDP policies are given in Fig. 12. It can be observed that the obtained storages from HSDP policy is not well matching with the perfect storages from DDP, especially the optimal May beginning storages obtained by HSDP is apparently higher than the perfect ones by DDP. For example, the obtained Ertan May beginning storage by HSDP policy is 1,181.5 m, which is 15 m higher than 1,166.5 m, the optimal perfect reservoir May beginning storage by DDP shown in Fig. 13. This is due to the fact that, HSDP policy doesn't utilize any anew forecasts during wet season as a hydrological state variable, which makes Ertan May beginning storages by HSDP deviate from the perfect ones. In contrast, the obtained storages hydrograph and May beginning storage by PSDP-GRR policy are reasonable, which are well matching with the perfect storages simulated by DDP, as illustrated from the values of NSSS for PSDP-GRR policy obtained as 0.93 in Table 5.

However, there is still 429 GWh of annual power production including 95 GWh in dry season and 334 GWh in wet season, to be improved for PSDP-GRR policy as compared to DDP policy (Table 5), which is derived from historical inflow time series. Its forecast lead-time is a year, so the posterior inflow transition probability and the forecast predictive probability matrix will get reduced to an identity matrix

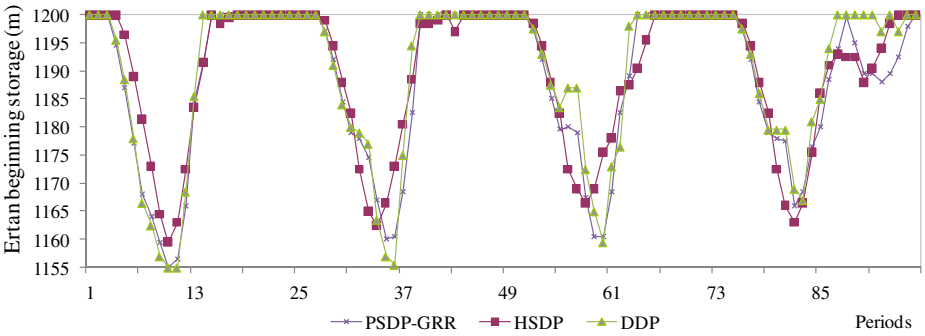

Fig. 12 Storage hydrograph obtained using PSDP-GRR, HSDP and DDP policies from 2003 to 2006

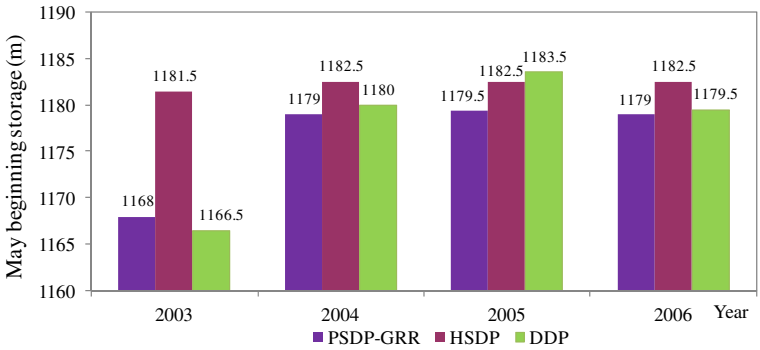

Fig. 13 The obtained Ertan May beginning storages by PSDP-GRR, HSDP and DDP policies from 2003 to 2006

for every stage. DDP policy is taking care of the carry over storage to meet the uncertainty of adequate inflow in the sequent periods and thus yielding better results. Compared with DDP policy for wet season, PSDP-GRR policy takes into account the forecasts of current period's inflow from a GRR model and the forecast predictive probability. The forecast lead-time of the GRR model is only one 10-day period, so the forecast predictive probability matrix is function of the prior inflow transition probability, but not an identity matrix. In this case, the forecast lead-time or the forecast predictive probability plays the governing role in PSDP-GRR model. To further increase the efficiency of power generation, the forecast lead-time has to be prolonged on the basis of improving the accuracy of the flood forecast for current period by making full use of available information on inflow or rainfall.

7 Summary and Conclusions

Forecasts of average areal precipitations for the next 10 days from Global Forecast System (GFS-QPFs) are evaluated to investigate the potential value in reservoir inflow forecasting and hydropower generation by revisiting the Ertan reservoir problem of the Yalong river basin comprehensively. A methodology for forecasting 10-day average inflow for current period using GFS-QPFs has also been presented and tested quantitatively, using a simple lumped hydrological model to estimate inflows from rainfall firstly. Then an improved Piecewise Stochastic Dynamic Programming model (PSDP) is finally proposed to generate operating policies for the Ertan station, to better off incorporate inflow forecasts with various lead-times as hydrologic state variables. Finally, performance of the PSDP model is compared with alternative stochastic programming models to evaluate the value of the QPFs from GFS in hydropower generation.

Inflow forecasts of 10-day average inflow are tested over a 5-year period on a 10-day basis during wet season, according to current operational practice, for the Ertan hydropower station. One of the most important results reported is given by comparing forecasts of 10-day average discharge with observed inflow and with results from the currently-used AR forecasting model, which makes no use of rainfall, whether observed or forecast. This comparison shows that the GRR model performs

better than the AR model, especially for low flows, both in terms of error statistics and of visual inspection of hydrographs and scatter plots.

An improved PSDP model is proposed to exploit the potential value of GFS-QPFs to long-term water system operations. Four performance indicators—Annual Total Hydropower Generation (ATHG), Nash–Sutcliffe Sufficiency Score (NSSS), reliability and vulnerability—are used to study the performance of the system under the policies and then to assist decision makers in selecting the best reservoir operating policy. As expected, the predicted inflows using the GRR model with GFS-QPFs result in better decisions with an increment of power generation as 114 GWh as compared with that using the AR model. In conclusion, the quantitative precipitation forecasts obtained by the Global Forecast System can be applied to 10-day average inflow forecasting and power generation scheduling of the Ertan hydropower station in the Yalong river basin. Further improvement of precipitation prediction skill on the meteorological side is needed and further work has to be done to tackle the uncertainty issue on the hydrological side.

Acknowledgements This research is supported by the National Natural Science Foundation of China (no. 50579095) and Ertan Hydropower Development Company, Ltd.

References

Anderson ML, Chen ZQ, Kavvas M, Feldman A (2002) Coupling HEC-HMS with atmospheric models for prediction of watershed runoff. J Hydrol Eng 7:312–318

Bartholmes J, Todini E (2005) Coupling meteorological and hydrological models for flood forecasting. Hydrol Earth Syst Sci 9(4):333–346

Beven KJ (2001) Rainfall–runoff modeling. The primer. Wiley, Chichester, p 360

Bremicker M, Homagk P, Ludwig K (2006) Early warning and forecast of floods in Baden-Wurtemberg. Wasserwirtschaft 7–8:46–50

Collischonn W, Haas R, Andreolli I, Tucci CEM (2005) Forecasting River Uruguay flow using rainfall forecasts from a regional weather-prediction model. J Hydrol 305:87–98

Collischonn W, Tucci CEM, Clarke RT et al (2007) Medium-range reservoir inflow predictions based on quantitative precipitation forecasts. J Hydrol 344:112–122

Doswell CA, Davies-Jones R, David LK (1990) On summary measures of skill in rare event forecasting based on contingency tables. Weather Forecast 5:576–585

Goweleeuw BT, Thielen J, Franchello G, De Roo APJ, Buizza R (2005) Flood forecasting using medium-range probabilistic weather prediction. Hydrol Earth Syst Sci 9(4):365–380

GRIB (2008) NCEP WMO GRIB2 documentation. Available at http://www.nco.ncep.noaa.gov/pmb/docs/grib2/

Habets F, LeMoigne P, Noilhan J (2004) On the utility of operational precipitation forecasts to served as input for streamflow forecasting. J Hydrol 293:270–288

Hashimoto T, Stedinger JR, Loucks DP (1982) Reliability,resiliency and vulnerability criteria for water resources system performance evaluation. Water Resour Res 18(1):14–20

Ibbitt RP, Henderson RD, Copeland J, Wratt DS (2000) Simulating mountain runoff with meso-scale weather model rainfall estimates: a New Zealand experience. J Hydrol 239:19–32

Jasper K, Gurtz J, Lang H (2002) Advanced flood forecasting in Alpine watersheds by coupling meteorological observations and forecasts with a distributed hydrological model. J Hydrol 267:40–52

Karamouz M, Vasiliadis HV (1992) Bayesian stochastic optimization of reservoir operation using uncertain forecasts. Water Resour Res 28(5):1221–1232

Kim YO, Palmer RN (1997) Value of seasonal flow forecasts in Bayesian stochastic programming. J Water Resour Plan Manage 123:327–335

Klemes V (1977) Discrete representation of storage for stochastic reservoir optimization. Water Resour Res 13(1):149–158

Koussis AD, Lagouvardos K, Mazi K, Kotroni V, Sitzmann D, Lang J, Zaiss H et al (2003) Flood forecasts for urban basin with integrated hydro-meteorological model. J Hydrol Eng 8(1):1–11

Krzysztofowicz R, Henry D (2001) Hydrologic uncertainty processor for probabilistic river stage forecasting: precipitation-dependent model. J Hydrol 249:46–68
Li PW, Lai EST (2004) Short-range quantitative precipitation forecasting in Hong Kong. J Hydrol 288:189–209
Maceira MEP, Damázio JM, Ghirardi AO, Dantas HM (1997) Use of periodic ARMA(p,q) models for weekly streamflow forecasts. In: Proceedings of the XII Brazilian water resources symposium, ABRH, Vitoria, ES
Mayer PL (1970) Introduction to probability and statistical applications. Oxford and IBH, New Delhi
McCuen RH (1998) Hydrologic analysis and design, 2nd edn. Prentice Hall, Englewood Cliffs
Moore RJ, Bell VA, Jones DA (2005) Forecasting for flood warning. Compt Rendus Geosci 337: 203–217
Pappenberger F,Beven KJ,Hunter NM, Bates PD et al (2005) Cascading model uncertainty from medium range weather forecasts (10 days) through a rainfall–runoff model to flood inundation predictions within the European Flood Forecasting System (EFFS). Hydrol Earth Syst Sci 9(4):381–393
Qiu RT, Wang BD, Zhou HC (2004) New idea for controlling the limited elevation of reservoirs in the flood season. Advances in Water Science 15(1):68–72
Rabuffetti D, Barbero S (2005) Operational hydro-meteorological warning and real-time flood forecasting: the Piemonte Region case study. Hydrol Earth Syst Sci 9(4):457–466
Reed S, Koren V et al (2004) Overall distributed model intercomparision project results. J Hydrol 298:27–60
Stedinger JR, Sule BE, Loucks DP (1984) Stochastic dynamic programming models for reservoir operation optimization. Water Resour Res 20(1 I):1499–1505
Sun NZ, Yang SL, Yeh WWG (1998) A proposed stepwise regression method for model structure identification. Water Resour Res 34(10):2561–2572
Suresh KR (2002) Modeling for irrigation reservoir operation. Ph.D. thesis, Department of Civil Engineering, Indian Institute of Science, Bangalore, India
Tejada-Guibert JA, Hohson S, Stedinger JR (1995) The value of hydrologic information in stochastic dynamic programming models of a multi-reservoir system. Water Resour Res 31(10):2571–2579
Vijaykumar V, Rao BV, Mujumdar PP (1996) Optimal operation of a multibasin reservoir system. Sadhana 21(4):487–502
Wang BD, Zhu YY, Zhang GH, Zhou HC (2005) Feasibility analysis of applying 24 h precipitation forecasts from the Central Meteorological Observatory. Journal of China Hydrology 25(6):30–34
Yeh W (1985) Reservoir management and operation models: a state of the art review. Water Resour Res 21(12):1797–1818
Young GK (1967) Findings reservoir operating rules. J Hydraul Div Am Soc Civ Eng 93(HY6): 297–321
Yu Z, Lakhtakia MN et al (1999) Simulating the river-basin response to atmospheric forcing by linking a mesoscale meteorological model and hydrologic model system. J Hydrol 218:72–91
Yuan JX, Wang BD, Wang FX, Li FW (2008) Study on real-time dynamic operation of reservoir level in flood season based on short-term rainfall forecast information. Journal of Hydroelectric Engineering 27(4):15–19
Zhang HG, Guo SL, Li CQ (2006) Preliminary analysis of uncertainty in quantitative precipitation forecast of TGP reservoir interval area. Yangtze River 37(4):39–41
Zhou HC, Wang F et al (2009) Study on the runoff description and optimal operation models for Ertan hydropower station. Journal of Hydroelectric Engineering 28(1):18–24
Zhu YJ (2007) Objective evaluation of global precipitation forecast. Available at http://www.emc.ncep.noaa.gov/gmb/yzhu/gif/pub/Zhu_QPF_VRFY.pdf